Biology of Reproduction, 2025, **112(5)**, 1015–1027
https://doi.org/10.1093/biolre/ioaf029
Advance access publication date 12 February 2025
Research Article

Duplex sequencing identifies unique characteristics of ENU-induced mutations in male mouse germ cells†

Danielle PM LeBlanc[1], Gu Zhou[1], Andrew Williams[1], Matthew J Meier[1], Charles C Valentine[2], Jesse J Salk[3], Carole L Yauk[4] and Francesco Marchetti[1,*]

[1]Environmental Health Science and Research Bureau, Health Canada, Ottawa, Ontario, Canada
[2]Fulcrum Genomics, Somerville, Massachusetts, USA
[3]Division of Hematology and Oncology, University of Washington School of Medicine, Seattle, Washington, USA
[4]Department of Biology, University of Ottawa, Ottawa, Ontario, Canada

*__Correspondence:__ Environmental Health Science and Research Bureau, Health Canada, 251 Sir Frederick Banting Driveway, Ottawa, Ontario K1A 0K9, Canada. E-mail: francesco.marchetti@hc-sc.gc.ca

†__Grant Support:__ Funding for this research was provided by Health Canada's Genomics Research and Development Initiative and the Chemicals Management Plan to FM. CLY gratefully acknowledges the Canada Research Chairs Program.

Abstract

Germ cell mutagenicity testing is increasingly required for chemical risk assessment. Duplex sequencing is rapidly gaining acceptance as a method to assess in vivo mutagenesis, and as a valid alternative to transgenic rodent mutation models such as the MutaMouse. We used a duplex sequencing panel of 20 genomic targets and the transgenic rodent assay to measure mutations in the germ cells of MutaMouse males exposed to 0, 1, 2, or 5 mg/kg *N*-ethyl-*N*-nitrosourea for 28 days. Germ cells from the seminiferous tubules were collected 28 days post-exposure. The transgenic rodent assay showed a significant increase in mutant frequencies at the high ($P < 0.001$) and medium ($P = 0.01$) *N*-ethyl-*N*-nitrosourea doses relative to controls, while duplex sequencing revealed a significant increase ($P < 0.001$) in *N*-ethyl-*N*-nitrosourea–induced mutations only at the high dose. Duplex sequencing mutation frequencies were lower in genic than in intergenic targets, suggesting a protective role for transcription-coupled repair. Interestingly, we observed several unique germ cell characteristics with respect to duplex sequencing data from rodent somatic tissues: 1) larger inter-animal variability in clonally expanded mutations that affects the ability to detect significant increases in mutation frequency; 2) a target on chromosome 2 showing much higher susceptibility to spontaneous and chemical-induced mutagenesis than other targets; and 3) a mutation spectrum consistent with that observed in the offspring of *N*-ethyl-*N*-nitrosourea–treated males but not with the spectrum in bone marrow of directly-exposed males. These results suggest that duplex sequencing is a promising approach for characterizing germ cell mutagenesis and that mutagenic mechanisms operating in germ cells differ from those in somatic tissues.

Received: October 15, 2024. **Revised:** January 21, 2025. **Accepted:** February 11, 2025

Graphical Abstract

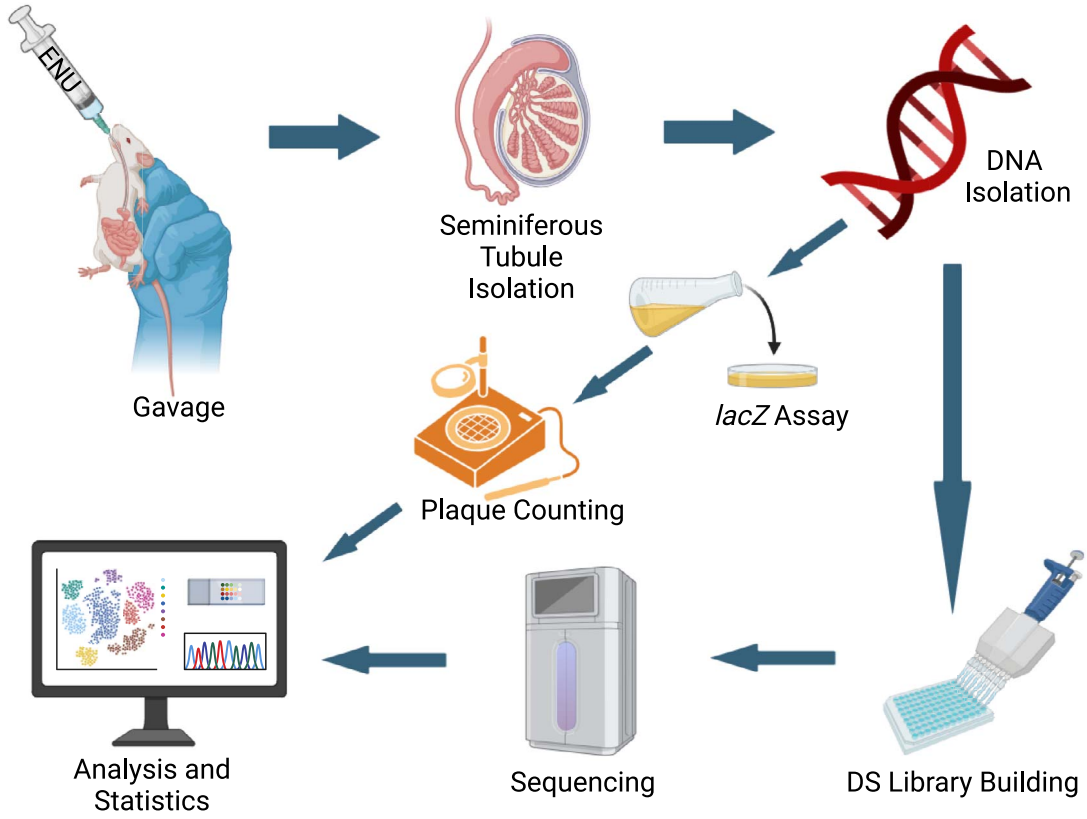

Key words: error-corrected sequencing, ecNGS, germ cells, mutation spectrum, MutaMouse, transgenic rodent assay, mutation susceptibility, benchmark dose modelling.

Introduction

Germline mutations can be detrimental to reproductive health and lead to diseases including autism, schizophrenia, and epilepsy, among others [1–4]. The last 50 years of research in germ cell mutagenesis have identified diverse environmental exposures that increase germline mutation rates [5–7]. Indeed, more than 80 agents have been shown to induce mutations in rodent germ cells [8]. A subset of these agents have been proposed as candidate human germ cell mutagens, such as ionizing radiation, tobacco smoke, polycyclic aromatic hydrocarbons, and other forms of air pollution [5]. However, a number of challenges hampered the advancement of our understanding of environmental exposures that cause germ cell mutagenicity [7]. One of these is the rarity of mutations in germ cells, which are one order of magnitude lower than in somatic tissues [9]. Thus, improved methods that are sufficiently sensitive and accurate are needed to better understand the relationship between germ cell mutagenesis and development of environmentally induced human genetic disease.

The transgenic rodent (TGR) gene mutation assay is the only Organisation for Economic Co-Operation and Development (OECD) test guideline (TG) that measures mutations in the germ cells of exposed rodents and represents the "gold-standard" for in vivo mutagenicity studies [10, 11]. The TGR assay uses bacterial reporter genes to measure mutations in vivo that result in loss of function through in vitro positive selection of recovered plasmids [12]. The assay has been used extensively for germ cell mutagenicity testing [13]; however, there are a number of limitations. First, it is a stand-alone assay requiring specialized rodent strains, which prevents its integration within standard toxicity testing. Second, the bacterial reporter gene used as the mutagenesis target is non-transcribed and not representative of the natural variability in native genomic features that may impact mutation susceptibility; third, the assay is limited to detecting mostly single nucleotide variants and 1–2 bp indels; lastly, transgene mutations must be individually recovered and sequenced from bacterial plaques to elucidate the mutation spectrum and to correct for clonally expanded mutations [14]. These TGR shortcomings limit its ability to generate results that fully inform the mutagenicity of test substances and evaluate their potential relevance to human mutation induction and disease development.

Advances in next-generation sequencing have pushed the boundaries of germ cell research and allowed for detailed investigations into the origin of de novo mutations (DNM). Whole genome sequencing (WGS) studies have consistently shown that DNM in human offspring increase with parental age and that the majority of single-nucleotide variants (SNV) DNM are paternal in origin [15–17]. Recently, extremely high levels of DNM have been observed in a few cases where the father had received chemotherapy prior to the child's conception [18]. In rodents, WGS studies have shown significant

increases in DNM in the offspring of male mice exposed to benzo[a]pyrene and ionizing radiation prior to conception [19, 20]. Therefore, both human and rodent data suggest that paternal preconception exposure to mutagenic agents can influence the DNM rate. However, WGS is not amenable to the study of mutations directly in male germ cells as these mutations are rare events that are masked by the inherently high error rate of current sequencing technologies.

Duplex sequencing (DS) is an error-corrected next-generation sequencing (ecNGS) technology that shows great potential for applications in mutagenesis research [21, 22]. DS increases the accuracy of mutation detection through unique labeling of each strand of DNA prior to sequencing [23]. To capture mutations, DS typically uses a panel of twenty 2.4 kb targets spread across autosomes encompassing genic and intergenic regions. The technology's low error rate and its ability to derive mutation frequency and spectra concurrently provides accurate and in-depth information on a test substance's mutational characteristics. Importantly, DS is applicable to any rodent model allowing the integration of mutagenicity assessment within standard toxicity studies that rely on wild type rodent [21, 22]. Studies with a variety of established mutagens have shown that DS detects dose-dependent increases in mutations in somatic tissues of rodents and produces chemical-specific mutation spectra consistent with known mechanisms [24–28]. These studies also demonstrate excellent concordance of DS and TGR mutation frequencies. Additionally, mouse DS studies show a higher susceptibility to mutation induction in intergenic regions relative to genic regions [25, 26]. Overall, these initial studies show that DS is effective at detecting chemically induced mutations in somatic tissues of rodents.

Application of ecNGS to germ cell mutation analysis is still limited to a few proof-of-principle studies. Bae *et al.* [29] detected a spontaneous mutation frequency of 2.72×10^{-8} in the sperm of a 39-year old-male using an ecNGS technology called Concatenating Original Duplex for Error Correction (CODEC). Salazar *et al.* [30] used DS to investigate the effect of age on spontaneous mutations in ∼4.5 kb of the coding region of *FGFR3*, the gene that causes achondroplasia [31], in the sperm of young and old men. Finally, Axelsson *et al.* [32] characterized mutations in the sperm of six healthy young men using DS and reported high concordance between mutation spectrum in sperm and inherited mutations in children. DS has yet to be applied to measure chemically induced mutagenesis in the germline.

Here, we used DS to detect *N*-ethyl-*N*-nitrosourea (ENU)-induced mutations in germ cells from the seminiferous tubules of MutaMouse male mice, a common TGR model. The objectives of our study were to: 1) investigate the dose-dependent increase in germline mutations following ENU exposure; 2) assess mutation frequencies across DS targets and identify features that increase mutation susceptibility; and 3) compare the DS results with those found in somatic tissues in previous work and with the gold-standard TGR assay.

Materials and methods

Animal exposure and tissue collection

All animal exposures, handling, and procedures were approved by the Health Canada Ottawa Animal Care Committee. MutaMouse mice from the in-house colony were maintained under a 12 h light/12 h dark photoperiod at a room temperature of 21°C and relative humidity of 50% with ad libitum access to water and food (Teklad Global 14% Rodent Maintenance Diet) for the duration of the study. Following OECD TG 488 recommendations [11], adult MutaMouse males ($n = 6$ per group), 9–14 weeks of age at the beginning of the exposure, were randomly assigned to dose groups of either 1, 2, or 5 mg/kg/day ENU, prepared fresh daily, or phosphate-buffered saline (as the vehicle control, VC). The top ENU dose was selected based on a pilot dose-range finding study to eliminate doses inducing excessive signs of toxicity. Mice received ENU or VC by oral gavage for a period of 28 consecutive days. As per OECD TG 488 [11], mice were euthanized 28 days following the final daily administration and the seminiferous tubules were collected as described [10]. Briefly, the seminiferous tubules were pressed out of the tunical albuginea and germ cells were released from the tubules using a tissue roller. The released germ cells were resuspended in Dulbecco phosphate-buffered saline, flash frozen, and stored at −80°C.

DNA extractions

Isolated germ cells from each mouse were processed by different DNA isolation protocols depending on the downstream mutation assay. To obtain the high-molecular weight DNA required for the TGR assay, the standard phenol-chloroform based DNA extraction method was used [10]. DNA for DS was isolated using the Qiagen DNeasy blood and tissue kits as described in the Qiagen user manual (Cat. # 69504, Qiagen, Hilden, Germany) with the following protocol modifications: the incubation step was set at 37°C degrees instead of 56°C degrees, 4 μL of RNAse solution was added, and the elution step was repeated twice with 40 μL of elution buffer.

TGR assay

Isolated DNA was used in the TGR assay as previously described [33]. Briefly, λgt10 phage vectors containing the bacterial *lacZ* gene were isolated from the genomic DNA and packaged into viable lambda phage particles using commercial packaging extract kits (Agilent Technology, Santa Clara, CA, USA). Phage particles were then used to infect *Escherichia coli* host cells (*lacZ*$^-$/*galE*$^-$), which were plated on either selective LB top agar containing 0.3% phenyl β-d-galactoside (P-gal; Sigma-Aldrich, Oakville, ON, Canada) or nonselective LB top agar. Following overnight incubation at 37°C, plaques were counted on both non-selective media plates (total plaque forming units) and selective media plates (mutants). Finally, mutant frequencies for each mouse were estimated by dividing the number of mutant plaques by the total plaque forming units.

DS library preparation

Isolated DNA was prepared for DS with the Mouse Mutagenesis Panel, which contains 20 targets spread across the mouse autosomes (2.4 kb each) as previously described [25]. Eleven of the 20 targets overlap intergenic regions and 9 overlap genic regions. The targets are reflective of the broader genome with respect to %GC-content and trinucleotide abundance, are void of repetitive elements and pseudogenes that could potentially confound alignment or variant calling, and were selected for optimal hybrid capture performance. The target regions have no known role in cancer development and are not known to be under positive or negative selection pressure.

An input of 1000 ng of isolated DNA was ultrasonically sheared to a mean fragment size of ~300 bp followed by end-polishing, A-tailing, and ligating to DS Adapters (Mouse Mutagenesis Kit, Version1.1, TwinStrand Biosciences Inc., Seattle WA, USA). Following the initial PCR amplification, the 48 kb of target regions included in the Mouse Mutagenesis Panel were enriched using a pool comprising 120-nucleotide biotinylated oligonucleotides in two tandem captures as previously described [25]. Libraries were shipped individually to Psomagen (Psomagen, Rockville MD, USA) for sequencing on a NovaSeq 6000 using an average of ~250 million raw reads per sample (Illumina, San Diego CA, USA). Sequence data in the form of demultiplexed FASTQ files were uploaded to the DNAnexus platform and processed through the TwinStrand Biosciences DuplexSeq Mutagenesis App (Version 3.20.1). Post-processed data files were provided though DNAnexus in the format of MUT files that were then processed through an in-house R pipeline.

The number of mutations were evaluated using two alternative approaches as previously described [26]. Briefly, under the conservative approach, all identical mutations within a sample were considered as deriving from a single independent event; the calculated minimum mutation frequency (MF_{min}) is the number of unique mutant duplex bases divided by the total number of duplex bases sequenced. Under a second approach, identical mutations within a sample were considered as deriving from separate independent events; thus, maximum mutation frequency (MF_{max}) is all mutant duplex bases divided by the total number of duplex bases sequenced.

Data processing and statistical analysis

All data processing and statistical analyses were conducted using R version 4.1.1. For both the TGR assay and DS, estimated MFs were obtained using generalized linear modelling (GLM) with a quasibinomial distribution followed by pairwise comparisons using the doBy R library according to the approach described by Højsgaard and Halekoh [34]. MFs by target locus were estimated using the generalized linear mixed modelling (GLMM) approach with a binomial error distribution. Pairwise comparisons based on transcription status were estimated using the doBy library. The delta method was used to approximate the standard error of the mean (SEM) of the estimated MFs by dose and by target. P-values were adjusted using the Holm–Sidak approach to account for multiple comparisons. A modified approach was used to identify differences in overall mutation spectra between treatment groups, as previously described [26, 35]. To account for differences in specific mutations subtypes individual GLMs were conducted for each substitution type independently.

MFs obtained with DS were compared to *lacZ* mutant frequencies using correlation analysis in Excel followed by benchmark dose (BMD) modelling using PROAST in R (version 70.1, https://rivm.nl/en/proast), as previously described [25]. The BMD gives an indication of chemical potency through fitting dose–response data to four mathematical models (Hill, exponential, reverse exponential, and lognormal) and generating 95% confidence intervals (CIs) for the dose at which a specified effect size occurs (called the benchmark response: BMR) [36, 37]. Since a standardized BMR has not been established for ecNGS studies, we selected a BMR of 50% based on recommendations by White *et al.* [38] and published DS studies [25, 26]. However, we also tested lower and higher BMRs. Specifically, we selected 60% as it is at the high end of what has been previously used for genotoxicity endpoints [38],10% as it is the approach currently used for standard toxicology dose–response analyses [39], and 20% as preliminary work suggests that it may be an appropriate BMR for ecNGS studies.

Power analyses

We performed a power analysis to determine the minimum sample size and total informative duplex bases needed to observe a significant increase in MF in male germ cells using DS using the approach previously described [40]. The power analyses were completed using in-house R scripts. First, we repeatedly generated random samples to simulate experiments for different sample sizes and different levels of sample-to-sample variability. Here, we used a binomial distribution to randomly generate control samples based on parameters from our experiment. Mutation counts were computer-generated based on average MFs in the control group and average bases sequenced per animal. A sample standard deviation of 0.22 was derived considering the standard deviation of each target estimated using GLMM. This estimate as well as values of 0.15, 0.2, 0.25, and 0.3 were used to simulate overdispersion in the population. This was done by modifying the baseline MF for each sample by adding simulated values assuming a normal distribution with mean zero with estimated and chosen standard deviation. To calculate the power of the analysis, a GLM was used to determine the significance between generated control and treated samples. A treatment group was generated following the same parameters with a selected fold-increase determined by the bisection method [41] for estimating the minimum detectable fold-change. Finally, we varied the sample size from 5, the minimum number of animals per group required by OECD TG 488, to 30 and assessed the power under these varied conditions.

Results

We used DS and the *lacZ* assay to measure ENU-induced germ cell mutations 28 days after the end of a 28-day exposure as per OECD TG 488. With this experimental design, mutations measured in germ cells collected from seminiferous tubules originated in cells that were stem cells and differentiating spermatogonia during the exposure [42]. ENU doses used in this study did not induce overt signs of toxicity and did not significantly affect testis weight at any of the doses tested with respect to controls (Supplementary Table 1).

DS metrics

We sequenced 24 DS libraries generated from germ cells of MutaMouse males exposed to ENU. DS read pairs were distributed evenly across samples with an average of ~327 million read pairs per sample. This resulted in an average duplex consensus depth of ~20,000× with an average of ~1.2 billion informative duplex bases screened for mutations per sample (Supplementary Figure 1A). All samples exceeded a minimum target of 500 million informative duplex bases (Supplementary Figure 1B).

DS MF_{min} and MF_{max} by dose

We calculated DS MF in two ways to assess the impact of clonally expanded mutations. Using the MF_{min} approach, we identified 725, 817, 902, and 1475 unique mutations and

Table 1. Mean DS mutation frequency estimates (MF_{min} and MF_{max}) and corresponding pairwise comparisons between ENU dose groups obtained using a Generalized Linear Modelling

Dose	MF_{min} assumption			MF_{max} assumption		
(mg/kg-bw/day)	Mean MF_{min} ± SEM ($x10^{-7}$)	Fold change	*P*-value*	Mean MF_{max} ± SEM ($x10^{-7}$)	Fold change	*P*-value*
0	1.19 ± 0.1			2.34 ± 0.1		
1	1.32 ± 0.1	1.11	0.52	2.20 ± 0.1	0.94	0.94
2	1.54 ± 0.1	1.29	0.20	2.00 ± 0.1	0.85	0.97
5	2.86 ± 0.2	2.39	6.7×10^{-6}	9.22 ± 0.3	3.94	0.12

*Bold font indicates adjusted $P < 0.05$.

MFs (± SEM × 10^{-7}) of 1.19 ± 0.1, 1.32 ± 0.1, 1.54 ± 0.2, 2.86 ± 0.2 in mice treated with VC, 1, 2, and 5 mg/kg-bw/day ENU, respectively (Table 1; Figure 1A). ENU induced a significant 2.4-fold increase in MF_{min} at the high dose relative to VC ($P < 0.001$). No significant effect was observed for the 1 and 2 mg/kg-bw/day ENU dose groups. Using the MF_{max} approach, we captured an additional 697, 543, 273, and 3281 mutations resulting in average MFs (× 10^{-7}) of 2.34 ± 1.31, 2.20 ± 1.25, 2.00 ± 1.23, 9.22 ± 2.81 for mice treated with VC, 1, 2, and 5 mg/kg-bw/day ENU, respectively (Table 1; Figure 1B). Hereafter, we will refer to mutations reported with the MF_{max} approach as putative clonal mutations since we cannot determine whether they may have arisen from a single event that was clonally expanded or from independent events at the same location. These putative clonal mutations were dispersed across genomic loci with a maximum of 139 clonally expanded mutations located at a single locus of a control sample, which consisted of a T:A > C:G mutation at genomic location 50835330 on chr2. Interestingly, 86% of the 4794 total clonally expanded mutations were found on the chromosome 2 target (chr2), and 60% of these were found in a single sample. A non-statistically significant 4.0-fold increase in MF_{max} was observed at 5 mg/kg-bw/day ENU dose group relative to VC, while MF_{max} for the two lower ENU doses were below the VC. The inclusion of clonally expanded mutations increased inter-individual variability in MF and obscured the ENU response; thus, clonally expanded mutations were not considered further for downstream analyses.

DS MF by target

We analyzed mutation induction across the 20 genomic targets, henceforth referred to by the chromosome on which they are located. There was a 5.2-fold difference between the target with the highest background MF_{min} (chr2: 3.27×10^{-7}) and the target with the lowest background MF_{min} (chr16: 6.27×10^{-8}). ENU induced a statistically significant increase in MF_{min} in 14 of the 20 genomic targets at the high dose relative to VC ($P < 0.05$; Figure 2). At the middle ENU dose, only the chr7 target showed a significant MF_{min} response, while no target showed a significant increase at the low ENU dose. Chr2 and chr19 were the most and least responsive targets for ENU-induced mutations at the high dose, respectively. In fact, ENU induced a MF_{min} of 7.80×10^{-7} at chr2, which was 5.4-fold higher than the MF_{min} at chr19 (1.46×10^{-7}). We observed similar fold differences for the low (4.3-fold) and middle (5.9-fold) ENU dose groups between the target with the highest (chr2) and lowest MF_{min} (low: chr16; middle: chr15). Overall, we found an approximately 5-fold difference in response among the targets for both spontaneous and ENU-induced mutations irrespective of the exposure with enhanced sensitivity identified at the chr2 locus.

Since both spontaneous and ENU-induced MF_{min} for chr2 were significantly higher than any other locus, we evaluated the impact of its inclusion on the observed results. When chr2 was removed from the analysis, a statistically significant increase in MF_{min} ($P < 0.001$) was still observed at the high dose, but no significant effect at the two lowest ENU doses as in the original analysis. These results show that the increase at the high dose is significant even when excluding this highly responding locus.

Next, we investigated the effect of genomic context on mutation induction. A 5.2-fold and 1.9-fold maximum difference was observed in MF_{min} between the highest and lowest responding targets among intergenic and genic regions, respectively. There was no significant difference in the background MF_{min} between intergenic ($1.04 \times 10^{-7} \pm 1.11 \times 10^{-8}$) and genic ($1.00 \times 10^{-7} \pm 1.08 \times 10^{-8}$) targets. However, intergenic targets were more susceptible to ENU-induced mutations than genic targets. Indeed, the top nine responding targets at the high dose of ENU were all located in intergenic regions and the bottom four responding targets were in genic regions (Figure 2). The MF_{min} was 1.7-fold higher ($P < 0.001$) in intergenic compared to genic regions in the high dose group, and 1.3-fold higher in the low dose group. No significant differences were observed between intergenic and genic regions in the middle dose group. Removing chr2 from the analysis reduced the fold-increase to 1.5 between intergenic and genic regions, but retained significance ($P < 0.001$) between intergenic and genic regions at the high ENU dose. Thus, the susceptibility of intergenic targets was not driven by the elevated response in the chr2 target. Overall, we found that intergenic targets are more susceptible to ENU-induced mutations than genic targets in germ cells.

Mutation spectra

Comparisons of spontaneous and ENU-induced mutation spectra indicated the induction of mainly SNVs. C:G > G:C transversions were the most common spontaneous mutation, with a MF 4.82×10^{-8}, followed closely by C:G > A:T and C:G > T:A substitutions (Figure 3). An initial pairwise comparison of the overall DS spectra showed a significant difference at all ENU doses relative to VC ($P < 0.001$). At the high dose, ENU significantly induced T:A > C:G mutations (MF_{min} 2.05×10^{-7}) followed by C:G > T:A (MF_{min} 9.82×10^{-8}) and T:A > A:T (MF_{min} 5.99×10^{-8}) ($P < 0.001$). C:G > G:C and C:G > A:T mutations were not significantly increased by the high ENU dose. Further investigation by each substitution

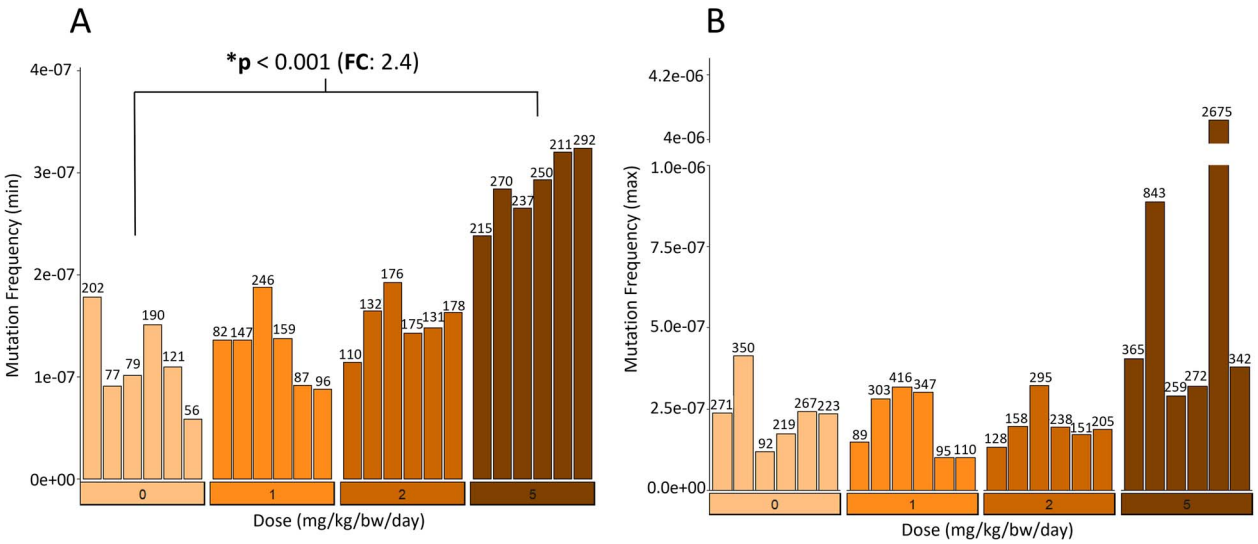

Figure 1. DS mutation frequencies in germ cells of MutaMouse males exposed to ENU. Data are presented as MF_{min} (A) and MF_{max} (B). Bars represent the respective MF (mutations per bp) for each animal. Numbers over the bars are the total mutation count per animal. The X-axes show the ENU dose (mg/kg-bw/day). In (A), the asterisk indicates a significant difference ($P < 0.001$) relative to the vehicle control in the average MF across animals the high ENU dose group. In (B), the ggbreak package was used to generate a break in the y-axis [58]. FC = fold change

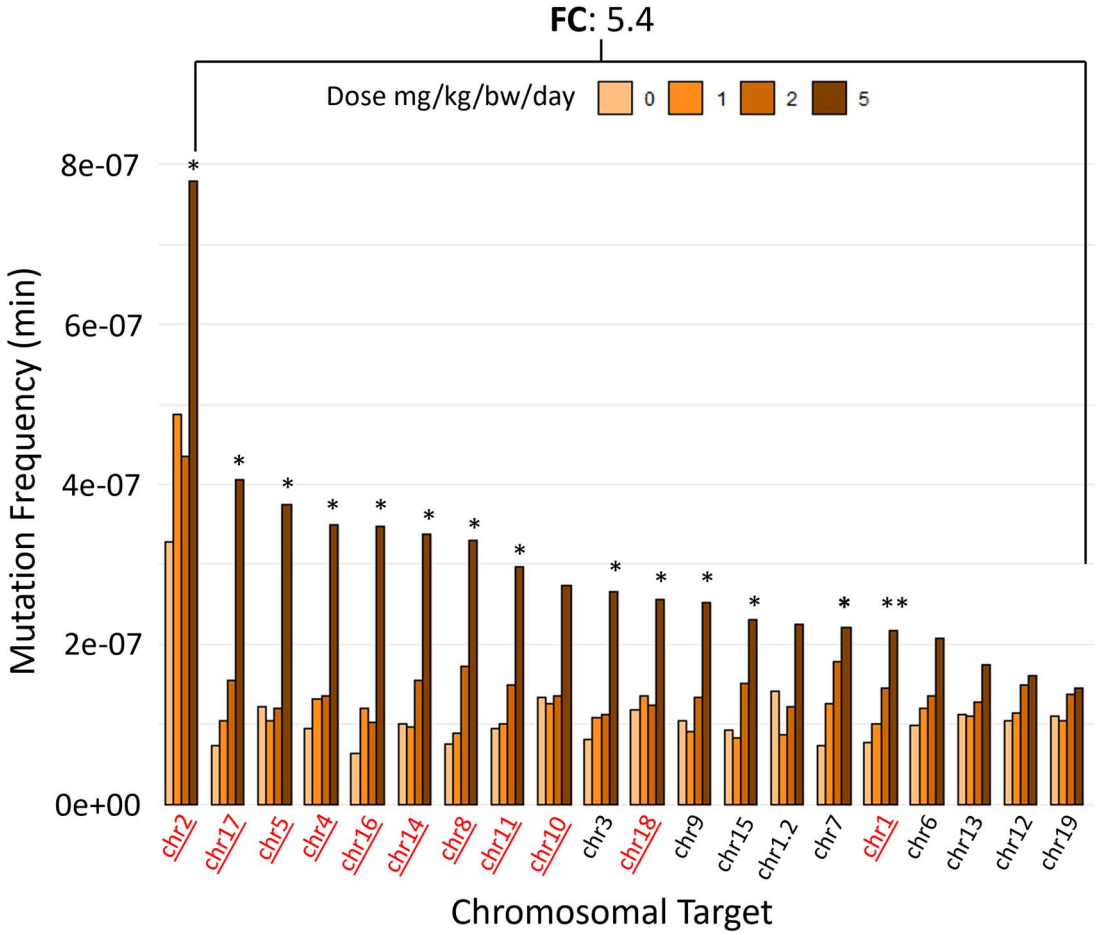

Figure 2. Spontaneous and ENU-induced MF by target using DS. The 20 targets in the Mouse Mutagenesis Panel are ordered from the highest MF_{min} at the high ENU dose (left) to the lowest MF_{min} (right). Data are mean MF_{min} (for each target, $n = 6$) separated by ENU dose (mg/kg-bw/day). Intergenic targets are underined. Asterisks indicate a significant increase ($P < 0.05$, generalized linear mixed model) at the high ENU dose relative to vehicle control. The double asterisk indicates a significant increase at the high and middle ENU doses relative to vehicle control. FC = fold change.

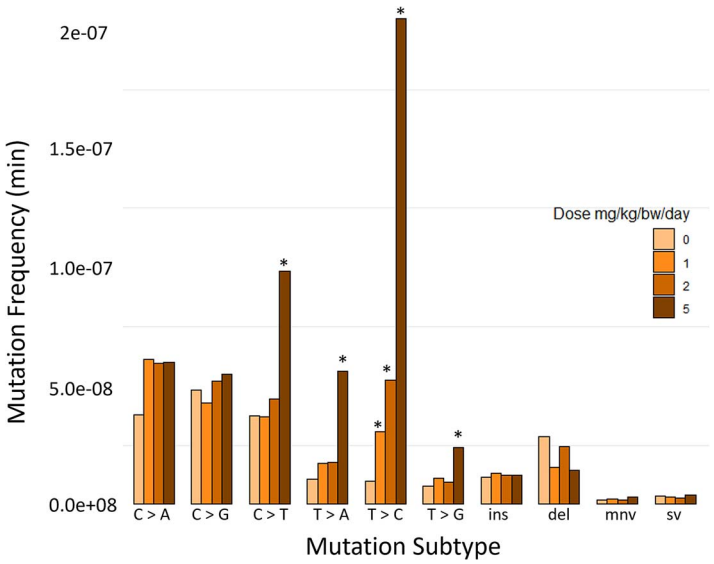

Figure 3. Mutation spectra of vehicle controls and ENU dose groups measured by DS in the germ cells of MutaMouse males. Mutation subtypes are presented as the average $MF_{min} \pm SEM$. Mutation subtypes include the six single nucleotide variants using a pyrimidine reference, small insertions (ins), small deletions (del), multinucleotide variants (mnv), and structural variants (sv). Asterisks indicate a significant increase ($P < 0.05$) in MF from vehicle controls.

type revealed that T:A > C:G transitions, the main type of mutation induced by ENU, were the only mutations significantly increased ($P < 0.001$) at the low and middle doses, with significant fold-changes in MF_{min} relative to VC of 3.1 and 5.2, respectively (Supplementary Table 2). Thus, DS is able to detect significant spectral changes in the germ cells following ENU exposure even in the absence of an overall increase in MF.

We compared the ENU spectrum in germ cells with that observed in the BM of Sprague–Dawley rats [28] and BigBlue mice [24] 28 days after a single exposure or exposure on days 1, 2 and 3 to 40 mg/kg ENU, respectively (Supplementary Figure 2). T:A > C:G transitions were the most common mutation in the current study making up approximately half of the SNV mutations with T:A > A:T transversions proportionally accounting for less than half of the T:A > C:G transitions. However, T:A > A:T transversions were as common as T:A > C:G transitions in both BM studies. Interestingly, the preponderance of T:A > C:G transitions over T:A > A:T transversions was also observed in the spectrum of DNMs in the offspring of ENU-exposed gpt-delta male mice estimated by whole exome sequencing [43] (Supplementary Figure 2). These results provide support for the accuracy of DS in detecting chemically induced mutations in germ cells, highlight subtle differences in the mutation spectra between germ cells and BM, and suggest minor biological differences in the response of germ cells and BM to ENU.

Recurrent mutations

We investigated the distribution of induced mutations across the 20 chromosomal targets to identify potential mutation hotspots. This analysis showed a relatively even distribution of mutations along the 20 targets (data not shown). However, we uncovered identical mutations that recurred at the same position in multiple animals. To define these recurrent mutations, we identified identical mutations present at the same position in at least one other animal at a low frequency (VAF < 1%). In total, there were 544 (14%) recurrent mutations out of the 3919 mutations observed in the study comprising 108 sequence changes. On average, 14%, 18%, 13%, and 12% of mutations occurred in at least one other animal within the 0, 1, 2, and 5 mg/kg ENU dose groups, respectively. The percentage of recurrent mutations, as defined above, present in each individual animal ranged from 2% to a maximum of 51% (Supplementary Table 3). There were 42 mutations that appeared in a minimum of three animals in the study, and 18 that appeared in at least 50% of the animals Figure 4A). One mutation in particular, a MNV (CAT > TAC) at position 50833383 on chr2, appeared in 15 out of 24 animals (3 control, 12 treated) suggesting that it is highly susceptible to both spontaneous and induced mutagenesis.

Since these recurrent mutations may represent either true hotspot mutations or technical artifacts, we evaluated whether they influenced the observed MF_{min}. Removing recurrent mutations from the data did not change the overall MF_{min} results (Figure 4B). Furthermore, the spectra of recurrent mutations differed between control and treated mice (Figure 4C). Indeed, C:G > T:A mutations were the main recurrent mutation type in control mice (28%), whereas T:A > C:G mutations were the most common recurrent mutation types in treated mice (33%) consistent with the overall control and ENU spectrum, respectively. In summary, the results of this analysis support that the observed recurrent mutations are true mutagenic events representing potential mutational hotspots.

TGR assay results and concordance with DS

We performed the TGR assay on the same animals used for DS to evaluate the concordance between the two methods. An average of $320{,}122 \pm 136{,}985$ plaque forming units (PFUs) per sample were analyzed with the TGR assay. We observed average MFs ($\pm$ SEM $\times 10^{-5}$) of 2.15 ± 0.5, 3.79 ± 0.7, 4.83 ± 0.7, 14.8 ± 1.3 in mice treated with VC, 1, 2 and 5 mg/kg-bw/day ENU, respectively (Table 2). Pairwise comparisons showed significant increases relative to VC for the high and middle ENU doses ($P < 0.01$) with the low dose

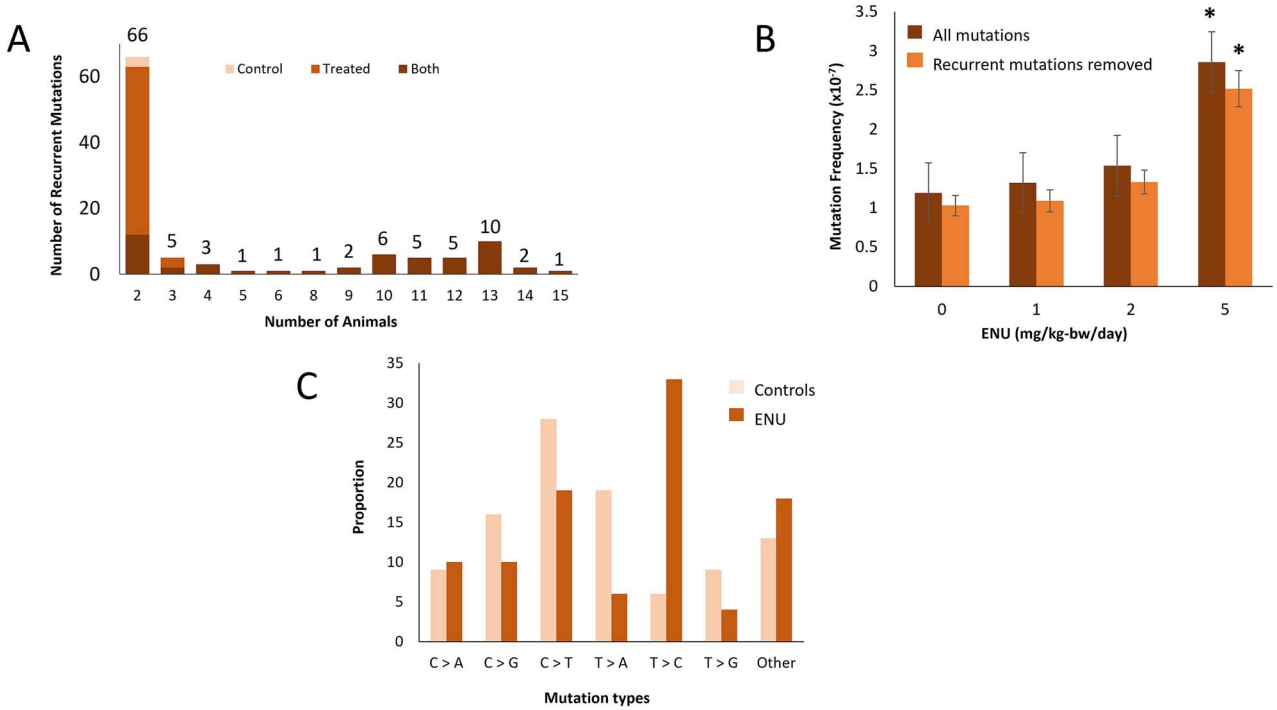

Figure 4. Impact of recurrent mutations on mutation spectra and mutation frequencies (MF_{min}) in vehicle controls and ENU dose groups measured by DS in the germ cells of MutaMouse males. (A) Distribution of recurrent mutations based on the number of animals affected. The color code identifies recurrent mutations that were observed only in vehicle controls, only in ENU-treated animals, or in both groups. (B) Average mutation frequencies (MF_{min}) by dose with and without recurrent mutations. The X-axis show the ENU dose (mg/kg-bw/day). Bars represent the SEM. (C) Proportion of mutation subtypes for the 32 and 90 recurrent mutations present among vehicle controls and treated mice, respectively. Other includes indels, mnv, and sv.

near the threshold for significance ($P = 0.052$). When the individual animals were considered, the Pearson correlation between the two assays was 0.78 (Figure 5A). However, when analyzed by dose, we found a very strong positive correlation between induced DS MF_{min} and TGR mutant frequencies (Pearson correlation; r = 0.998; Figure 5B). We also used the BMD approach to quantitatively compare the two assays. Although the magnitude of response was at least 2-fold higher in the TGR assay relative to DS MF_{min}, the BMDs estimated to elicit a 50% increase in mutations relative to VC for the two methods had overlapping 95% CI (Figure 5C). These were 2.3 mg/kg-bw/day (95% CIs of 1.3–3.6 mg/kg-bw/day) and 0.81 mg/kg-bw/day (95% CIs of 0.31–1.6 mg/kg-bw/day) for DS and *lacZ* assay, respectively. When the BMR was adjusted to either 10%, 20% or 60%, the CIs of the two assays still overlapped (Supplementary Table 4). Furthermore, when single targets were considered, the CIs of 11 out of 13 targets for which we could generate BMDs also overlapped with the *lacZ* assay (Figure 5C). We could not generate BMDs for seven targets as there was no dose–response trend in the data when analyzed individually.

Power analyses

We performed power analyses to assess the sensitivity of the DS and *lacZ* assays based on the number of animals and the observed standard deviations in this study (0.22 for DS and 0.20 for *lacZ*). To follow the OECD TG 488 requirement, we considered the minimal detectable fold-change when 5 mice per group are used. For DS, a 2-fold increase with 80% power is the minimal detectable fold-change that can be achieved when using a sample size of 5 mice per group and a standard deviation of 0.22 (Figure 6A). For the *lacZ* assay, the minimum detectable fold-change is 2.3-fold using a sample size of 5 mice per group and a standard deviation of 0.20 (Figure 6B). For detecting a 1.5-fold change (FC) at the standard deviation observed in this study, 13–14 animals would be required for DS and 19–20 animals would be required for the TGR assay. Thus, DS can detect a lower fold increase than the *lacZ* assay with fewer animals, despite having a higher animal-to-animal variation.

Table 2. Mean mutant frequency estimates and corresponding pairwise comparisons between ENU dose groups for the *lacZ* assay obtained using a Generalized Linear Modelling.

Dose (mg/kg-bw/day)	Mutant frequency ± SEM ($\times 10^{-5}$)	Fold Change (± SEM)	*P*-value*
0	2.15 ± 0.5		
1	3.79 ± 0.6	1.76 ± 0.5	5.24×10^{-2}
2	4.83 ± 0.7	2.24 ± 0.6	1.00×10^{-2}
5	14.8 ± 1.2	6.87 ± 1.6	1.68×10^{-7}

*Bold font indicates adjusted *P*-value <0.05

Discussion

We show that DS can be used to accurately measure chemically induced mutations in mouse germ cells. We observed a significant increase in MF_{min} at the high ENU dose of 5 mg/kg-bw/day relative to VC and that intergenic DS targets were more susceptible than genic targets to ENU-induced mutations in germ cells. ENU induced mainly T:A > C:G

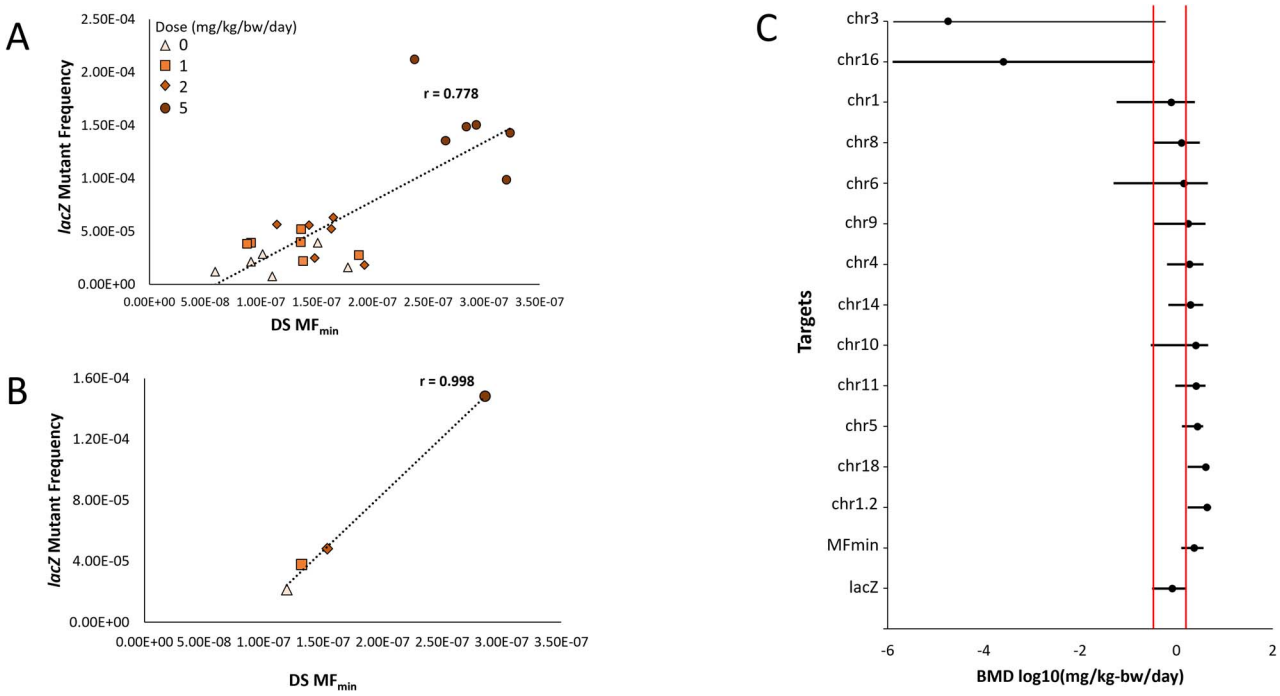

Figure 5. Comparison of DS and *lacZ* results. (A) Pearson correlation analysis between the *lacZ* assay and DS in the germ cells of MutaMouse males exposed to ENU by individual animal (A) and by dose (B). Data are presented as mutant frequencies for the *lacZ* assay, and as MF_{min} for DS. (C) Comparison of 95% CI based on BMD model averaging analyses between DS and the *lacZ* assay. The plot shows the log10 BMD for a 50% increase in *lacZ* mutant frequency and the DS MF_{min}. For DS, the overall BMD (MF_{min}) and those of the individual targets that could be modeled are shown. DS targets are organized from the lowest BMD to highest. The two vertical lines represent the CI for the *lacZ* assay.

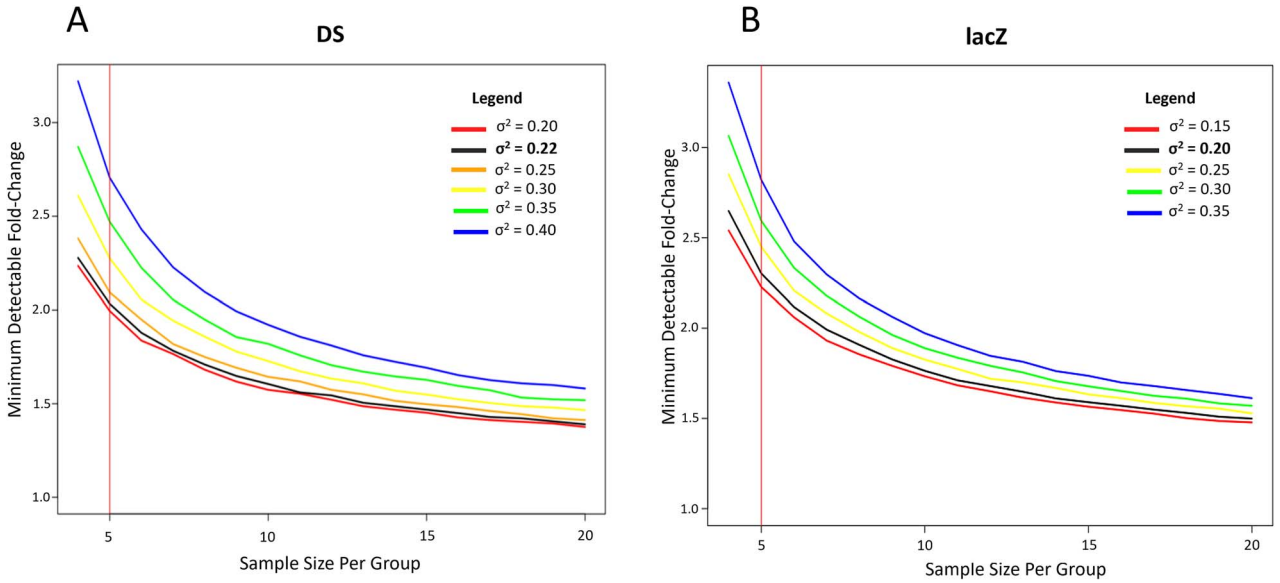

Figure 6. Power curves showing the minimum detectable FC with 80% power by DS MF_{min} (A) and the *lacZ* assay (B). The vertical line indicates the minimum number of animals per dose required by OECD TG 488 to conduct a valid test with the Transgenic Rodent Gene Mutation assay. The different curves indicate the variance values modeled, including the variance observed in our study (0.20).

transitions, followed by C:G > T:A transitions, which differs with what was observed in somatic cells [24, 28]. Comparison of DS results to the TGR assay performed on the same samples demonstrated a strong positive correlation at the dose group level. Our results identify germ cell unique mutagenic mechanisms and support the use of DS for assessing mutagenicity in male germ cells. Our findings also highlight the advantages of measuring mutagenesis in a variety of genomic targets to assess mutation susceptibility across the genome.

DS demonstrates variability in mutation susceptibility among genomic targets

One of the advantages of the DS panel used in this study compared with the TGR assay is the ability to identify genomic features that are associated with mutation susceptibility. Here, in a panel comprising twenty 2.4 kb regions, we observed a 5-fold difference in sensitivity across targets. The variability seen across these regions emphasizes the importance of querying

multiple regions to obtain a measure of the variability in susceptibility across different genomic feature. For example, we observed an increased susceptibility to ENU-induced mutations in intergenic relative to genic targets. This has been observed in other studies in somatic cells using DS [25, 26] and other methods [44, 45]. We previously proposed that a protective effect of transcription-coupled repair explained the higher MF_{min} in intergenic targets in the BM of mice exposed to benzo[a]pyrene, a bulky adduct-forming chemical [25], or to procarbazine, a methylating chemotherapeutic agent [26]. ENU-induced adducts are primarily repaired by O6-methylguanine-DNA methyltransferase (MGMT), also referred to as alkyl-guanine transferase (AGT) [46]. Repair by MGMT/AGT is not coupled to transcription [46]; however, nucleotide excision repair, which is coupled to transcription, also plays an important role in the repair of ENU adducts [46, 47], and other alkylating agents [48]. Therefore, we hypothesize that transcription-coupled nucleotide excision repair is of the factors involved in the higher susceptibility of intergenic DS regions to mutation induction in germ cells.

Two of the intergenic targets in the present study, i.e. chr16 and chr17, are among the top five most responsive in the BM of benzo[a]pyrene [25], procarbazine [26], and benzo[b]fluoranthene [49] exposed mice. In addition, the top five most responsive targets in the present study, namely chr2, 17, 5, 4, 16 and in previous work in the BM, namely chr14, 11, 8, 17, and 16, are all intergenic. This further supports a role for transcription-coupled repair pathways in modulating mutation susceptibility. These results suggest that there are genomic regions that are particularly susceptible to mutation induction across tissues and chemicals. Understanding the reasons for this increased susceptibility is an area for future investigation.

In this study, increased susceptibility to mutations was particularly apparent for chr2 in both controls and exposed groups. This appears to be a germ cell-specific response, as chr2 did not show spontaneous or chemically induced hypermutability in somatic tissues [25, 26]. Chr2 is intergenic and within heterochromatin; both these features have been associated with increased MFs in previous DS work [25, 26]. However, this is unlikely to explain the heightened susceptibility of this target in germ cells as the same target in bone marrow was not hypermutated. The GC content of the chr2 target appears to be in the middle range relative to other targets in the panel and there are no known hypermutable loci along the chr2 target, as shown in previous work [25]. Thus, further work is required to identify tissue-specific features that may contribute to the high susceptibility of the chr2 target in germ cells, including understanding potential tissue-specific differences in the transcriptional status of the targets.

Overall, the variability in mutation susceptibility across targets, the heightened response observed in intergenic regions relative to genic regions across chemical exposures, and the germ cell specific response of a single target highlights the importance of measuring mutagenesis across a diverse target panel rather than a single non-transcribed bacterial gene as is normally done with the TGR assay.

Mutation spectra analysis suggests a germ cell specific mutagenic mechanism

Another advantage of DS over the TGR assay is the simultaneous generation of MF and spectra to inform the underlying mutagenic mechanisms of the substance under investigation. ENU is a prototypical alkylating mutagen with a well characterized mode of action and spectrum [50]. ENU transfers its ethyl group to oxygen or nitrogen atoms on the four DNA bases, with particular affinity for the N7 position of guanine, O6 of guanine, O2 of thymine, N3 of adenine, and O2 of cytosine [51]. In mammals, MGMT/AGT is efficient at repairing O6-ethyl guanine adducts and less efficient at repairing adducts at O4-ethyl thymine [47]. Here, we observed primarily T:A > C:G transitions that arise from misrepair of O4-ethyl thymine adducts. This is consistent with what was observed in the BM of Sprague–Dawley rats [28] and Big-Blue mice [24]. However, we also observed differences in the proportions of the other types of mutations between BM and germ cells. These results suggest that although ENU induces the same types of mutations across tissues and species, the relative contribution of each mutation type appear to differ between BM and germ cells. Subtle differences in the mutation spectra of BM and germ cells were previously reported for benzo[a]pyrene exposure in the MutaMouse [52]. These data point to potential differences in DNA damage responses between somatic cells and germ cells.

An interesting observation in our study is that MF_{min} of T:A > C:G transitions were significantly increased with respect to VC at the low and middle ENU doses in the absence of a significant increase in the overall MF_{min}. T:A > C:A are the main types of mutations induced by ENU and limiting the analyses to this mutation type provides higher sensitivity to detect an effect. The findings support that statistical analysis of specific base substitution types could be used to determine whether the results of an experiment should be considered positive when dealing with weak effects. This would be similar to what is presently done with the Ames test, where multiple strains each detecting a specific mutation type are used and a positive result with a single strain is sufficient to conclude that the test chemical is mutagenic [53].

Validation of the ENU spectrum in germ cells obtained with DS is provided by the comparison with the spectrum of inherited mutations in the offspring of ENU-treated male mice [43]. This analysis showed good agreement in terms of the proportions of the various mutation types observed in germ cells versus those reported in the offspring. This finding shows that DS accurately detects germ cell mutations and provides strong support for its use to identify germ cell mutagens and estimate heritable mutagenic risk.

Recurrent mutations appear at low frequencies and do not impact MFs

The detailed site-specific information provided by DS allowed us to investigate the occurrence of hotspots, that is, locations at where mutations are present in multiple animals. We observed that about 3% of the unique mutations were present in multiple animals and about 40% of those were recurrent in at least three mice. Importantly, we found that the spectrum of recurrent mutations in treated mice is enriched for T:A > C:G mutations, which are the main type of mutation induced by ENU, while they are rare among the recurrent mutations in controls. This, along with the low frequency at which these mutations were observed (VAF < 1%) suggests that these are true events induced by ENU exposure rather than cross-contamination. Finally, the exclusion of recurrent mutations from the data did not change the outcome of the study.

The ability to identify these occurrences across genomic loci and determine their impact on MF through detailed spectra analysis is an additional advantage of the DS technology over existing TGR methods.

Clonality in germline tissue

Unlike the TGR assay, DS can differentiate unique and clonally expanded mutations allowing calculation of both MF_{min} (unique) and MF_{max} (clonally expanded). In previous work using DS in BM [25, 26], the inclusion of clonally expanded mutations did not change the overall conclusions and increased the correlation with the *lacZ* assay [25, 26]. In this study, we observed overlapping BMD CIs with the TGR assay using MF_{min}; however, when clonal mutations were considered, there was no longer a significant effect of ENU on MF. In fact, MF_{min} provided clear separation of the mice in the high ENU dose group with respect to the other groups in the study; however, when MF_{max} is considered, mice from controls, low and middle ENU doses have MF_{max} overlapping those in the high dose ENU group. The impact of clonal mutations was particularly evident in two mice in the high dose group that had significantly more clonally expanded mutations than any other animals; this result was largely driven by clonally expanded mutations on chr2. These results suggest a testis-specific impact of clonal mutations on the mutagenic response that is likely driven by the uniqueness of the spermatogenic process.

The formation of millions of mature sperm relies only on a small pool of spermatogonial stem cells (SSCs). In rodents, SSCs comprise only 0.03% of all germ cells in the testis [54]. Hematopoietic stem cells (HSCs) also comprise a very small proportion (0.01%–0.03%) of the cells they produce in the BM [55]. However, a major difference is the number of cell divisions required to produce differentiated/mature cells. During spermatogenesis, there are approximately 12 divisions occurring between SSC and completion of the two meiotic divisions, which yields approximately 4000 mature sperm from one SSC [56]. Conversely, in the BM, HSCs undergo 3–5 divisions resulting in as low as 8 mature cells produced from one HSC [57]. Following maturation, hematopoietic cells are released from the BM into the blood stream almost immediately. In contrast, maturing germ cells remain in the testes for several weeks [42]. Thus, in the testis, a mutation induced in a single SSC can expand to a larger number of cells and mutated germ cells continue to accumulate within the testis at each division of that SSC. Both these spermatogenic characteristics may explain the larger impact of clonality found in the germ cells relative to BM. These results suggest that DS studies of chemically induced mutagenesis in germ cells should focus on MF_{min}.

Comparison to the TGR assay

Although we have outlined the many advantages of DS, it is crucial to compare its results to the TGR assay, the current "gold-standard" for in vivo mutagenicity studies. We observed a strong correlation in mutation frequencies and BMD values between the two assays. It is possible that plaque sequencing may further improve the ability to adjust for clonal expansion in the *lacZ* assay to more accurately define mutant frequency and improve its concordance with DS. Finally, power analyses showed that DS and the *lacZ* assay can detect a 2- and a 2.3-fold increase when using the same number of animals per group, respectively. Together with the results published previously on somatic tissues [24–26, 28], these findings show that DS is a viable alternative to TGR assays for generating mutagenicity data for regulatory evaluations.

Conclusions

The ability to detect single nucleotide mutations in vivo in the male germline has been limited to an OECD approved test that has drawbacks. ecNGS technologies provide the opportunity to transform how germline mutagenesis is assessed. We demonstrate that DS can be used to measure chemically induced mutagenesis in germ cells to produce results that are comparable to the TGR assay. Importantly, DS provides additional detailed information that extends our understanding of the potential health implications of germ cell exposures. Specifically, the mutation spectrum information in this study suggests small but significant differences between germ cell and somatic tissue in the response to ENU. The observation of a single, germ cell-specific target with heightened sensitivity, and a higher overall susceptibility of intergenic targets, highlights the added benefit of measuring mutagenesis across multiple targets and not a single exogenous locus. Further work is required to identify features that influence tissue-specific susceptibility in germ cells. Overall, DS shows exceptional potential as an alternative method for evaluation of germline mutagenesis with many additional advantages over established methods.

Acknowledgments

The authors thank the team at TwinStrand Biosciences including Lindsey N. Williams and Zachary K. Norgaard for their work and continuous bioinformatics and administrative support. Additionally, the authors thank Julie Buick of Health Canada for her work on contract requirements for work completion.

Author contributions

Conceptualization: FM, CLY; Investigation: DPML, GZ; Formal analysis: DPML, GZ, AW, MJM, CCV, JJS; Resources: FM; Data curation: DLPM, GZ, AW; Writing—original draft preparation: DL, FM; Writing—review and editing: all authors; Funding acquisition: FM; Supervision: FM.

Conflict of interest: DPML, GZ, MJM, AW, CLY, and FM declare that they have no competing interests. CCV, and JJS declare that they were employees and equity holders at TwinStrand Biosciences Inc. at the time these experiments were initiated and are authors on one or more duplex sequencing-related patents.

Supplementary material

Supplementary Material is available at *BIOLRE* online.

Data availability

Sequencing data have been deposited with the Sequence Read Archive (SRA) under BioProject ID PRJNA1153588.

Sequencing data processing and bioinformatics analyses were performed on the DNAnexus platform using the TwinStrand Biosciences DuplexSeq Mutagenesis App (Version 3.20.1; https://platform.dnanexus.com/app/twinstrandbio-mutagenesis). Per-target mutation frequency calculation was performed using an R script (Supplementary materials).

Disclaimer

Health Canada does not endorse or recommend the products or services of any commercial entity, including TwinStrand Biosciences, Inc.

Ethical approval and consent to participate

The use and handling of laboratory animals in this study was approved by the Health Canada Ottawa Animal Care Committee under protocols 2011-020 and 2014-016. Methods were carried out in compliance with relevant Canadian guidelines and regulations.

References

1. Michaelson JJ, Shi Y, Gujral M, Zheng H, Malhotra D, Jin X, Jian M, Liu G, Greer D, Bhandari A, Wu W, Corominas R, *et al.* Whole-genome sequencing in autism identifies hot spots for de novo germline mutation. *Cell* 2012; **151**:1431–1442.
2. Li S, DeLisi LE, McDonough SI. Rare germline variants in individuals diagnosed with schizophrenia within multiplex families. *Psychiatry Res* 2021; **303**:114038.
3. Turner TN, Coe BP, Dickel DE, Hoekzema K, Nelson BJ, Zody MC, Kronenberg ZN, Hormozdiari F, Raja A, Pennacchio LA, Darnell RB, Eichler EE. Genomic patterns of de novo mutation in simplex autism. *Cell* 2017; **171**:710–722.e12.
4. Howrigan DP, Rose SA, Samocha KE, Fromer M, Cerrato F, Chen WJ, Churchhouse C, Chambert K, Chandler SD, Daly MJ, Dumont A, Genovese G, *et al.* Exome sequencing in schizophrenia-affected parent–offspring trios reveals risk conferred by protein-coding de novo mutations. *Nat Neurosci* 2020; **23**:185–193.
5. DeMarini D. Declaring the existence of human germ-cell mutagens. *Env Mol Mutagen* 2012; **53**:166–172.
6. DeMarini D. The mutagenesis moonshot: the propitious beginnings of the environmental mutagenesis and genomics society. *Env Mol Mutagen* 2019; **61**:8–24.
7. Singer T, Yauk C. Germ cell mutagens: risk assessment challenges in the 21st century. *Env Mol Mutagen* 2010; **51**:919–928.
8. Marchetti F, Douglas GR, Yauk CL. A return to the origin of the EMGS: rejuvenating the quest for human germ cell mutagens and determining the risk to future generations. *Environ Mol Mutagen* 2020; **61**:42–54.
9. Milholland B, Dong X, Zhang L, Hao X, Suh Y, Vijg J. Differences between germline and somatic mutation rates in humans and mice. *Nat Commun* 2017; **8**:15183.
10. O'Brien J, Beal MA, Gingerich JD, Soper L, Douglas GR, Yauk CL, Marchetti F. Transgenic rodent assay for quantifying male germ cell mutant frequency. *J Vis Exp* 2014; **90**:e51576.
11. OECD. Test No. 488: Transgenic Rodent Somatic and Germ Cell Gene Mutation Assays. In: *OECD Guidel. Test. Chem. Section 4*. Paris, France: OECD; 2022.
12. Lambert I, Singer T, Boucher S, Douglas G. Detailed review of transgenic rodent mutation assays. *Mutat Res* 2005; **590**:1–280.
13. Marchetti F, Aardema MJ, Beevers C, van Benthem J, Godschalk R, Williams A, Yauk CL, Young R, Douglas GR. Identifying germ cell mutagens using OECD test guideline 488 (transgenic rodent somatic and germ cell gene mutation assays) and integration with somatic cell testing. *Mutat Res Toxicol Environ Mutagen* 2018; **832-833**:7–18.
14. Beal MA, Meier MJ, LeBlanc DP, Maurice C, O'Brien JM, Yauk CL, Marchetti F. Chemically induced mutations in a Muta mouse reporter gene inform mechanisms underlying human cancer mutational signatures. *Commun Biol* 2020; **3**:1–11.
15. Conrad D, Keebler JE, DePristo M, Lindsay SJ, Zhang Y, Casals F, Idaghdour Y, Hartl CL, Torroja C, Garimella KV, Zilversmit M, Cartwright R, *et al.* Variation in genome-wide mutation rates within and between human families. *Nat Genet* 2011; **43**:712–714.
16. Rahbari R, Wuster A, Lindsay SJ, Hardwick RJ, Alexandrov LB, Al Turki, Dominiczak A, Morris A, Porteous D, Smith B, Stratton MR. Timing, rates and spectra of human germline mutation. *Nat Genet* 2015; **48**:126–133.
17. Shojaeisaadi H, Schoenrock A, Meier MJ, Williams A, Norris JM, Palmer ND, Yauk CL, Marchetti F. Mutational signature analyses in multi-child families reveal sources of age-related increases in human germline mutations. *Commun Biol* 2024; **7**:1–12.
18. Kaplanis J, Ide B, Sanghvi R, Neville M, Danecek P, Coorens T, Prigmore E, Short P, Gallone G, McRae J, Genomics England Research Consortium, Moutsianas L, *et al.* Genetic and chemotherapeutic influences on germline hypermutation. *Nature* 2022; **605**:503–508.
19. Adewoye AB, Lindsay SJ, Dubrova YE, Hurles ME. The genome-wide effects of ionizing radiation on mutation induction in the mammalian germline. *Nat Commun* 2015; **6**:6684.
20. Beal MA, Meier MJ, Williams A, Rowan-Carroll A, Gagné R, Lindsay SJ, Fitzgerald T, Hurles ME, Marchetti F, Yauk CL. Paternal exposure to benzo(a)pyrene induces genome-wide mutations in mouse offspring. *Commun Biol* 2019; **2**:228.
21. Marchetti F, Cardoso R, Chen CL, Douglas GR, Elloway J, Escobar PA, Harper T Jr, Heflich RH, Kidd D, Lynch AM, Myers MB, Parsons BL, *et al.* Error-corrected next generation sequencing—promises and challenges for genotoxicity and cancer risk assessment. *Mutat Res Mutat Res* 2023; **792**:108466.
22. Marchetti F, Cardoso R, Chen CL, Douglas GR, Elloway J, Escobar PA, Harper Jr T, Heflich RH, Kidd D, Lynch AM, Myers MB, Parsons BL, *et al.* Error-corrected next-generation sequencing to advance nonclinical genotoxicity and carcinogenicity testing. *Nat Rev Drug Discov* 2023; **22**:165–166.
23. Kennedy SR, Schmitt MW, Fox EJ, Kohrn BF, Salk JJ, Ahn EH, Prindle MJ, Kuong KJ, Shen JC, Risques RA, Loeb LA. Detecting ultralow-frequency mutations by duplex sequencing. *Nat Protoc* 2014; **9**:2586–2606.
24. Valentine CC, Young RR, Fielden MR, Kulkarni R, Williams LN, Li T, Minocherhomji S, Salk JJ. Direct quantification of in vivo mutagenesis and carcinogenesis using duplex sequencing. *Proc Natl Acad Sci U S A* 2020; **117**:33414–33425.
25. LeBlanc DPM, Meier M, Lo FY, Schmidt E, Valentine C III, Williams A, Salk JJ, Yauk CL, Marchetti F. Duplex sequencing identifies genomic features that determine susceptibility to benzo(a)pyrene-induced in vivo mutations. *BMC Genomics* 2022; **23**:542.
26. Dodge AE, LeBlanc DPM, Zhou G, Williams A, Meier MJ, van P, Lo FY, Valentine III CC, Salk JJ, Yauk CL, Marchetti F. Duplex sequencing provides detailed characterization of mutation frequencies and spectra in the bone marrow of Muta mouse males exposed to procarbazine hydrochloride. *Arch Toxicol* 2023; **97**:2245–2259.
27. Bercu JP, Zhang S, Sobol Z, Escobar PA, van P, Schuler M. Comparison of the transgenic rodent mutation assay, error corrected next generation duplex sequencing, and the alkaline comet assay to detect dose-related mutations following exposure to N-nitrosodiethylamine. *Mutat Res Toxicol Environ Mutagen* 2023; **891**:503685.
28. Smith-Roe SL, Hobbs CA, Hull V, Todd Auman J, Recio L, Streicker MA, Rivas MV, Pratt GA, Lo FY, Higgins JE, Schmidt EK, Williams LN, *et al.* Adopting duplex sequencing technology for genetic toxicity testing: a proof-of-concept mutagenesis experiment with N-ethyl-N-nitrosourea (ENU)-exposed rats. *Mutat Res Toxicol Environ Mutagen* 2023; **891**:503669.
29. Bae JH, Liu R, Roberts E, Nguyen E, Tabrizi S, Rhoades J, Blewett T, Xiong K, Gydush G, Shea D, An Z, Patel S, *et al.* Single duplex DNA sequencing with CODEC detects mutations with high sensitivity. *Nat Genet* 2023; **55**:871–879.
30. Salazar R, Arbeithuber B, Ivankovic M, Heinzl M, Moura S, Hartl I, Mair T, Lahnsteiner A, Ebner T, Shebl O, Pröll J, Tiemann-Boege I. Discovery of an unusually high number of de novo mutations in sperm of older men using duplex sequencing. *Genome Res* 2022; **32**:499–511.
31. Chen J, Yu C, Zhao Y, Niu Y, Zhang L, Yu Y, Wu J, He J. A novel non-invasive detection method for the FGFR3 gene mutation

in maternal plasma for a fetal achondroplasia diagnosis based on signal amplification by hemin-MOFs/PtNPs. *Biosens Bioelectron* 2017; **91**:892–899.
32. Axelsson J, LeBlanc D, Shojaeisaadi H, Meier MJ, Fitzgerald DM, Nachmanson D, Carlson J, Golubeva A, Higgins J, Smith T, Lo FY, Pilsner R, *et al.* Frequency and spectrum of mutations in human sperm measured using duplex sequencing correlate with trio-based de novo mutation analyses. *Sci Rep* 2024; **14**:23134.
33. Marchetti F, Zhou G, LeBlanc D, White PA, Williams A, Yauk CL, Douglas GR. The 28 + 28 day design is an effective sampling time for analyzing mutant frequencies in rapidly proliferating tissues of Muta mouse animals. *Arch Toxicol* 2021; **95**:1103–1116.
34. Højsgaard S, Halekoh U. *Package 'do By': Groupwise Statistics*. Linear Estimates, Utilities: LSmeans; 2023.
35. Piegorsch WW, Bailer AJ. Statistical approaches for analyzing mutational spectra: some recommendations for categorical data. *Genetics* 1994; **136**:403–416.
36. Wills JW, Long AS, Johnson GE, Bemis JC, Dertinger SD, Slob W, White PA. Empirical analysis of BMD metrics in genetic toxicology part II: in vivo potency comparisons to promote reductions in the use of experimental animals for genetic toxicity assessment. *Mutagenesis* 2016; **31**:265–275.
37. Wills JW, Johnson GE, Battaion HL, Slob W, White PA. Comparing BMD-derived genotoxic potency estimations across variants of the transgenic rodent gene mutation assay. *Environ Mol Mutagen* 2017; **58**:632–643.
38. White PA, Long AS, Johnson GE. Quantitative interpretation of genetic toxicity dose-response data for risk assessment and regulatory decision-making: current status and emerging priorities. *Environ Mol Mutagen* 2020; **61**:66–83.
39. Johnson GE, Soeteman-Hernández LG, Gollapudi BB, Bodger OG, Dearfield KL, Heflich RH, Hixon JG, Lovell DP, MacGregor JT, Pottenger LH, Thompson CM, Abraham L, *et al.* Derivation of point of departure (PoD) estimates in genetic toxicology studies and their potential applications in risk assessment. *Environ Mol Mutagen* 2014; **55**:609–623.
40. Esina E, Dodge AE, Williams A, Schuster DM, LeBlanc DPM, Marchetti F, Yauk CL. Power analyses to inform duplex sequencing study designs for Muta mouse liver and bone marrow. *Environ Mol Mutagen* 2024; **65**:234–242.
41. Burden RL, Faires JD. *Numerical Analysis*. Boston, Mass: Prindle, Weber & Schmidt; 1985.
42. Marchetti F, Aardema M, Beevers C, van Benthem J, Douglas GR, Godschalk R, Yauk CL, Young R, Williams A. Simulation of mouse and rat spermatogenesis to inform genotoxicity testing using OECD test guideline 488. *Mutat Res Toxicol Environ Mutagen* 2018; **832–833**:19–28.
43. Masumura K, Ando T, Toyoda-Hokaiwado N, Ukai A, Nohmi T, Honma M. Comparison of the frequencies of ENU-induced point mutations in male germ cells and inherited germline mutations in their offspring. *Genes Environ* 2021; **43**:43.
44. Xia B, Yan Y, Baron M, Wagner F, Barkley D, Chiodin M, Kim SY, Keefe DL, Alukal JP, Boeke JD, Yanai I. Widespread transcriptional scanning in the testis modulates gene evolution rates. *Cell* 2020; **180**:248–262.e21.
45. Chapman MA, Lawrence MS, Keats JJ, Cibulskis K, Sougnez C, Schinzel AC, Harview CL, Brunet JP, Ahmann GJ, Adli M, Anderson KC, Ardlie KG, *et al.* Initial genome sequencing and analysis of multiple myeloma. *Nature* 2011; **471**:467–472.
46. Bronstein SM, Cochrane JE, Craft TR, Swenberg JA, Skopek TR. Toxicity, mutagenicity, and mutational spectra of N-ethyl-N-nitrosourea in human cell lines with different DNA repair phenotypes. *Cancer Res* 1991; **51**:5188–5197.
47. Tosal L, Comendador MA, Sierra LM. In vivo repair of ENU-induced oxygen alkylation damage by the nucleotide excision repair mechanism in Drosophila melanogaster. *Mol Genet Genomics MGG* 2001; **265**:327–335.
48. Ozturk S, Demir N. DNA repair mechanisms in mammalian germ cells. *Histol Histopathol* 2011; **26**:505–517.
49. Schuster DM, LeBlanc DPM, Zhou G, Meier MJ, Dodge AE, White PA, Long AS, Williams A, Hobbs C, Diesing A, Smith-Roe SL, Salk JJ, *et al.* Dose-related mutagenic and clastogenic effects of benzo[b]fluoranthene in mouse somatic tissues detected by duplex sequencing and the micronucleus assay. *Environ Sci Technol* 2024; **58**:21450–21463.
50. Stottmann R, Beier DR. ENU mutagenesis in the mouse. *Curr Protoc Hum Genet Editor Board Jonathan Haines Al* 2014; **82**:15.4.1-15.4.10.
51. Beranek DT. Distribution of methyl and ethyl adducts following alkylation with monofunctional alkylating agents. *Mutat Res* 1990; **231**:11–30.
52. O'Brien JM, Beal MA, Yauk CL, Marchetti F. Next generation sequencing of benzo(a)pyrene-induced lacZ mutants identifies a germ cell-specific mutation spectrum. *Sci Rep* 2016; **6**:36743.
53. OECD. Test No. 471: Bacterial Reverse Mutation Test. In: *OECD Guidelines for the Testing of Chemicals, Section 4*. Paris: OECD Publishing.
54. Aponte PM. Spermatogonial stem cells: current biotechnological advances in reproduction and regenerative medicine. *World J Stem Cells* 2015; **7**:669–680.
55. Challen GA, Boles N, Lin KK, Goodell MA. Mouse hematopoietic stem cell identification and analysis. *Cytom Part J Int Soc Anal Cytol* 2009; **75A**:14–24.
56. Fayomi AP, Orwig KE. Spermatogonial stem cells and spermatogenesis in mice, monkeys and men. *Stem Cell Res* 2018; **29**:207–214.
57. Seita J, Weissman IL. Hematopoietic stem cell: self-renewal versus differentiation. *Wiley Interdiscip Rev Syst Biol Med* 2010; **2**:640–653.
58. Xu S, Chen M, Feng T, Zhan L, Zhou L, Yu G. Use ggbreak to effectively utilize plotting space to deal with large datasets and outliers. *Front Genet* 2021; **12**:774849.

Biology of Reproduction, 2025, 112(5), 1015–1027
https://doi.org/10.1093/biolre/ioaf029
Research Article